[2]I. M. Cheshire, Proc. Phys. Soc. (London) 83, 227 (1964).
[3]J. C. Y. Chen and M. H. Mittleman, Ann. Phys. (N. Y.) 37, 264 (1966).
[4]M. F. Fels and M. H. Mittleman, Phys. Rev. 163, 129 (1967).
[5]B. H. Bransden and Z. Jundi, Proc. Phys. Soc. (London) 92, 880 (1967).
[6]C. K. Majumdar and A. K. Rajagopal, Phys. Rev. 184, 144 (1969).
[7]J. F. Dirks and Y. Hahn, Phys. Rev. A 2, 1861 (1970).
[8]J. F. Dirks and Y. Hahn, Phys. Rev. A 3, 310 (1971).
[9]Y. Hahn, Phys. Rev. C 1, 12 (1970).
[10]C. Schwartz, Phys. Rev. 124, 1468 (1961).
[11]A. K. Bhatia, A. Temkin, R. J. Drachman, and H. Eiserike, Phys. Rev. A 3, 1328 (1971).
[12]P. G. Burke and K. Smith, Rev. Mod. Phys. 34, 473 (1962).
[13]F. E. Harris, Phys. Rev. Letters 19, 173 (1967).
[14]R. K. Nesbet, Phys. Rev. 179, 60 (1969).
[15]K. Smith, Proc. Phys. Soc. (London) 78, 549 (1961).
[16]G. J. Seiler, R. S. Oberoi, and J. Callaway, Phys. Rev. A 3, 2006 (1971).
[17]R. J. Damburg and E. Karule, Proc. Phys. Soc. (London) 90, 637 (1967).
[18]P. G. Burke, D. F. Gallaher, and S. Geltman, J. Phys. B 2, 1142 (1969).
[19]W. J. Cody, J. Lawson, H. S. Massey, and K. Smith, Proc. Roy. Sco. (London) A278, 479 (1964).
[20]M. Rotenberg and J. Stein, Phys. Rev. 182, 1 (1969).
[21]R. J. Drachman, Phys. Rev. 144, 25 (1966).
[22]S. E. Wakid and R. W. LaBahn, Phys. Letters 35A, 151 (1971).
[23]S. Geltman and P. G. Burke, J. Phys. B 3, 1062 (1970).

PHYSICAL REVIEW A VOLUME 6, NUMBER 6 DECEMBER 1972

Screening Effects in Atomic Pair Production below 5 MeV*

H. K. Tseng and R. H. Pratt
Department of Physics, University of Pittsburgh, Pittsburgh, Pennsylvania 15213
(Received 22 June 1972)

Quantitative predictions for atomic-electron screening effects in low-energy pair production follow from the knowledge that the small-distance shape of screened-electron and positron continuum wave functions is close to that of point-Coulomb wave functions of shifted energy. These predictions are verified by making exact numerical calculations in representative cases. The energy-shift normalization theory is then used in conjunction with the point-Coulomb results of Øverbø to obtain predictions for atomic-pair-production energy distributions and total cross sections for photon energies from threshold to 5 MeV. Atomic-electron screening effects cause appreciable modifications of the total cross sections for photon energies below 1.5 MeV and continue to have a major effect on some portions of the energy distribution at higher photon energies. Results are also compared with Bethe–Heitler predictions and with experiments.

With the continuing improvements in computers it is becoming feasible to make fairly accurate theoretical calculations of atomic-pair-production cross sections in the low-energy region where the Bethe–Maximon[1] high-energy results and Born approximation[2] (the well-known Bethe–Heitler formula) need not be valid. Relativistic calculations of pair production in a point-Coulomb-potential model have now been reported by Øverbø, Mork, and Olsen (ØMO); more extensive results have been given by Øverbø.[3] This use of a point-Coulomb model relies on the expectation, based on form-factor estimates,[4] that the effects of atomic-electron screening would be unimportant in this energy region. Such an estimate is obtained because the maximum impact parameter r_{max} discussed by Heitler,[5] equal to q_{min}^{-1} with $q_{min} = k - p_+ - p_-$, is of the order of the electron Compton wavelength and is quite small compared to the radius of the atom. However, we subsequently performed the lengthy relativistic calculations[6] of pair-production cross sections in screened potentials and found that, near threshold, atomic-electron screening effects are important. At electron-Compton-wavelength distances an electron sees a point-Coulomb potential corresponding to the nuclear charge Z. The electron wave function has a hydrogenlike shape; the only effect of atomic-electron screening, as described by a central potential V deviating from the point-Coulomb form, is to modify the normalization. For a very-low-energy continuum wave function (but not for higher energies) this normalization is indeed sensitive to the screening. We showed in fact that we could roughly obtain screened pair-production cross sections from point-Coulomb cross sections simply by using a multiplicative normalization factor.

We have recently examined[7] in greater detail the

shapes of electron wave functions near, but outside, the atomic nucleus. This leads to a more quantitative prediction of the effect of atomic-electron screening on pair-production cross sections, in the entire energy range of the point-Coulomb calculations of ØMO and Øverbø.[3] Our observation was that a screened-electron or positron wave function of shifted energy $\delta E_{\pm} = \pm V_0$ (plus sign for positron and minus sign for electrons) at small distances is even closer in shape to a point-Coulomb wave function than is a screened wave function of the same energy (i.e., $\delta E_{\pm} = 0$). Here $\delta E \equiv E - E_c$ (the subscript c stands for the point-Coulomb potential case $V_c = -a/r$, with $a = Z\alpha$), and we assume the central potential $V = -(a/r + V_0 + \tilde{V})$, with $\tilde{V}(r=0) = 0$; V_0 is a constant. An analytic calculation indicated that the deviation from the point-Coulomb shape at small distances is approximately[7]

$$\frac{\alpha^2 Z^{4/3} \gamma^2}{(2l+3)} \quad \text{for } \delta E_{\pm} = 0$$

and

$$\frac{\alpha^3 Z^{5/3} \gamma^3}{6(l+2)} \quad \text{for } \delta E_{\pm} = \pm V_0 \text{ for } l\text{th partial waves.}$$

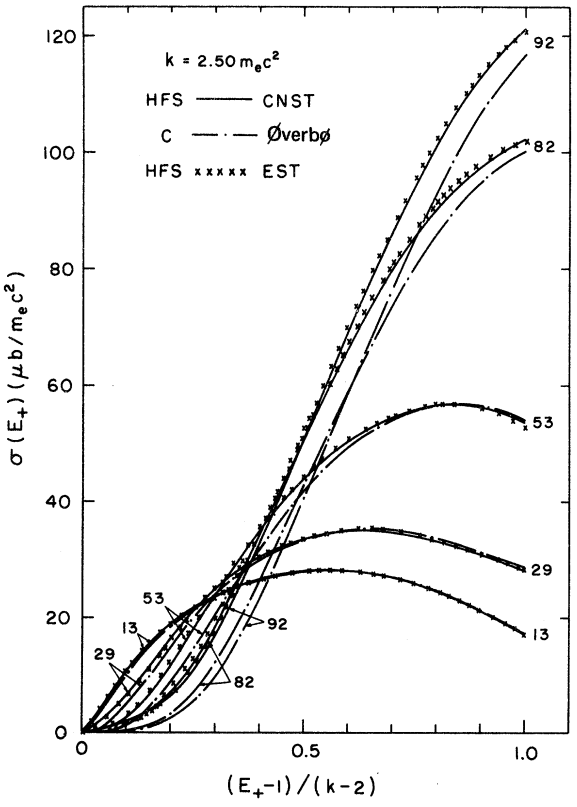

FIG. 1. Comparison of pair-production cross sections $\sigma(E_+)$ for $k = 2.50\, m_e c^2$ with the Kohn-Sham (HFS) potential and the point-Coulomb (c) potential. The numbers attached to the curves give the atomic number of the target element.

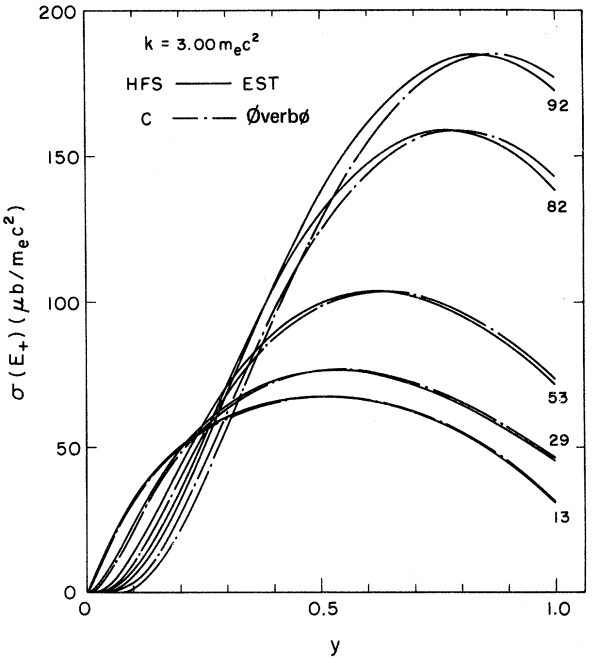

FIG. 2. Same as Fig. 1 except that the photon energy k is $3.00\, m_e c^2$.

This has been verified in numerical calculations. Since the energy shifts for electron and positron are equal and opposite, we predict that a point-Coulomb pair-production angular distribution with a specified split (E_+, E_-) of photon energy $k = E_+ + E_-$ between the pair differs only by a normalization factor from the screened distribution resulting from the same photon energy k but split $(E_+ + V_0, E_- - V_0)$ between the positron and electron. We also noted a simple behavior of the continuum-state normalization. For low-κ partial waves, except at very low energies,[7] $\tilde{N}_s \equiv (p_s E_s)^{1/2} N_s$ is equal to $\tilde{N}_c \equiv (p_c E_c)^{1/2} N_c$ for the case with energy shift, where N_s and N_c are the normalizations of the wave functions of screened and point-Coulomb potentials, respectively. At high energies even for high-κ partial waves $\tilde{N}_s = \tilde{N}_c$ with or without energy shift. For atomic pair production,[6] the low-κ partial waves dominate the cross section for low photon energies. Consequently for photon energies above about 1.2 MeV we predict the relation

$$\sigma_s(E_+ + V_0, E_- - V_0) = \sigma_c(E_+ + E_-)$$

between screened and point-Coulomb pair-production energy distributions. Our purpose in this paper is to use numerical data to test the validity of this prediction and then, once established, to use the prediction to obtain screened results over the full range of the ØMO and Øverbø point-Cou-

TABLE I. Comparisons of the shape of pair-production angular cross sections without energy shift $\delta E_+ = E_{+s} - E_{+c} = 0$ and with energy shift $\delta E_+ = -0.03 \cong V_0 \cong -0.0321\ m_e c^2$ for $Z = 92$, $k = 2.10\ m_e c^2$. Symbols s and c refer to the Kohn–Sham and the point-Coulomb potentials, respectively $[\sigma(E_+, y) \equiv Z^{-2}\, d\sigma/dE_+ \equiv \sigma(E_+)]$.

θ_+ (deg)	$\frac{\sigma^s(E_+, \theta_+, y=0.6)}{\sigma^c(E_+, \theta_+, y=0.6)} \Big/ \frac{\sigma^s(E_+, y=0.6)}{\sigma^c(E_+, y=0.6)}$	$\frac{\sigma^s(E_+, \theta_+, y=0.3)}{\sigma^c(E_+, \theta_+, y=0.6)} \Big/ \frac{\sigma^s(E_+, y=0.3)}{\sigma^c(E_+, y=0.6)}$
0	1.175	1.013
10	1.166	1.010
20	1.142	1.003
30	1.109	0.994
40	1.074	0.984
50	1.042	0.978
60	1.014	0.976
70	0.990	0.978
80	0.971	0.984
90	0.955	0.994
100	0.944	1.004
110	0.938	1.016
120	0.935	1.028
130	0.935	1.040
140	0.937	1.050
150	0.939	1.062
160	0.940	1.071
170	0.941	1.078
180	0.941	1.080

lomb calculations.

For very low photon energies where $\tilde{N}_s \neq \tilde{N}_c$, say, $k = 2.1 m_e c^2$ to $2.3 m_e c^2$, the main region of importance for the atomic-pair-production matrix element is the region of space[6] where $r \sim \frac{1}{2}$, while with increasing energy the important region grows. For $r \sim \frac{1}{2}$ the screening effect[7] on the shape of the continuum-state wave function is still very small even without energy shift, i.e., $\delta E_\pm = 0$. In our previous work[6] we used the ratio of dominant partial-wave normalizations (without energy shift) to convert all the point-Coulomb results of ØMO and Øverbø for incident-photon energies in the range $2.1 m_e c^2 - 2.6 m_e c^2$. This theory was verified by our numerical calculations in this photon-energy range. In principle we can now obtain better angular distributions with the energy-shift theory. But in practice, for very low energies the energy shift is large enough that most points (E_+, E_-) of the energy spectrum are shifted to unphysical points of the point-Coulomb spectrum (negative electron kinetic energy). Thus, in this photon-energy range, we use the results obtained previously for the pair-production cross sections $\sigma(E_+)$ and σ, where $\sigma(E_+) \equiv Z^{-2} d\sigma/dE_+$ is the energy distribution, and σ is the total cross section. However, we show one example of the application of the energy-shift theory to prediction of very-low-photon-energy pair-production angular distributions

$$\sigma(E_+, \theta_+, y) \equiv Z^{-2} \frac{d\sigma}{dE_+ d\Omega_+} ,$$

with and without energy shift, in Table I. We can see that the shape of the angular distributions is improved with the energy shift, especially in the regions $30° - 120°$ of primary importance for the integrated result $\sigma(E_+)$. (The deviations at small and large angles are probably not real, as more partial waves are required for an accurate numerical calculation at these angles.)

For higher photon energies, say $k = 2.6 m_e c^2$ to $10.0 m_e c^2$, we can test the energy-shift screening theory (EST) prediction of the relation between cross sections. We anticipate that this screening theory is good to about 1% for photon energy from $2.5 m_e c^2$ to $10 m_e c^2$, because the minimum momentum transfer $q_{\min} = k - (k^2 - 4)^{1/2}$ varies from 2 to

TABLE II. Comparison of the total pair-production cross section σ with the energy-shift screening theory (EST) and with the corrected-effective-normalization screening theory (CNST), for photon energy $k = 2.5$ and $2.6\ m_e c^2$ with the Kohn–Sham (HFS) potential.

k $(m_e c^2)$	Z	$\sigma^{\mathrm{HFS}}_{\mathrm{CNST}}$ (mb/atom)	$\sigma^{\mathrm{HFS}}_{\mathrm{EST}}$ (mb/atom)
2.50	13	1.85	1.86
	29	10.9	11.0
	53	50.7	51.0
	82	168	169
	92	228	230
2.60	18	5.66	5.62
	82	252	253
	92	351	352

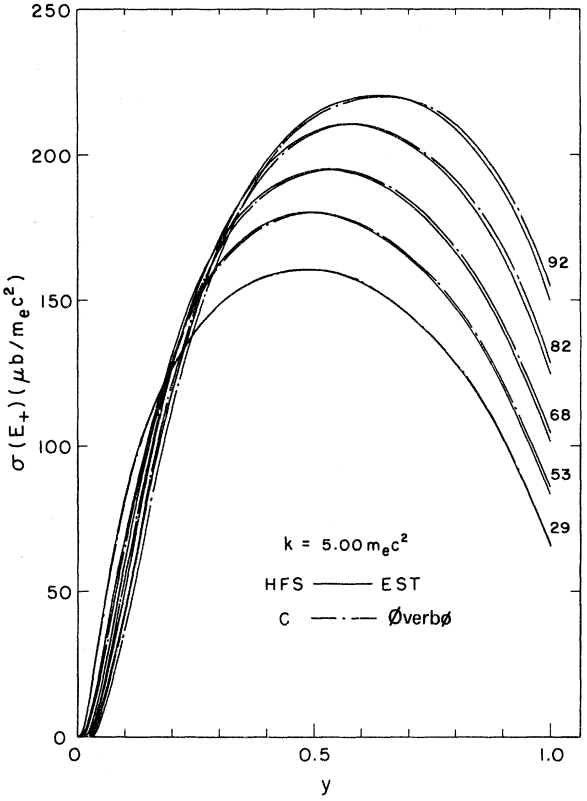

FIG. 3. Same as Fig. 1 except that the photon energy k is 5.00 $m_e c^2$.

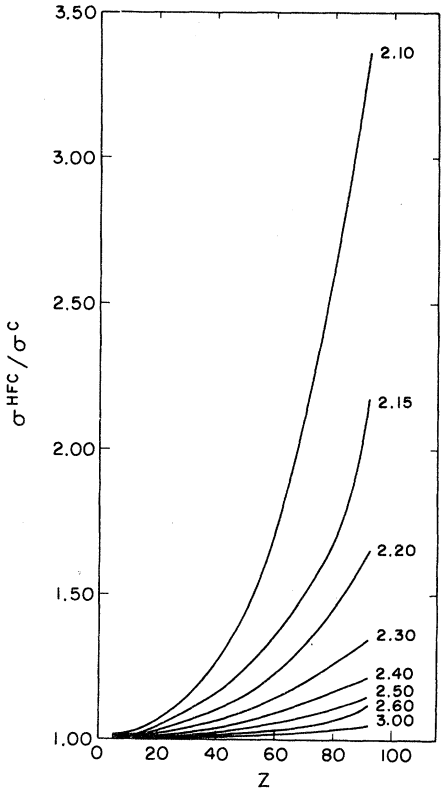

FIG. 5. Values of the atomic-electron screening factors σ^{HFS}/σ^c. The numbers attached to the curves give the incident photon energy k in $m_e c^2$ units.

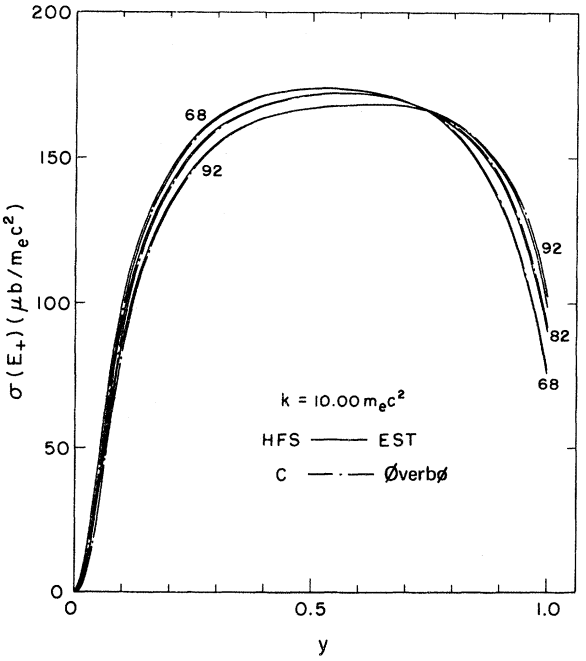

FIG. 4. Same as Fig. 1 except that the photon energy k is 10.00 $m_e c^2$.

0.2 over this range, and at the corresponding distance $r_{max} \equiv q_{min}^{-1}$, the shapes of point-Coulomb and energy-shifted screened wave functions are still close. (At higher energies this will not be true.) Further, the energy is high enough that $(p_s E_s)^{1/2} N_s = (p_c E_c)^{1/2} N_c$. We present the energy distribution of the pair-production cross section of the Kohn–Sham [Hartree–Fock–Slater with two-thirds Slater's exchange (HFS)] potential[8] for the photon energy $k = 2.5$ in Fig. 1. It agrees very well with that previously calculated with an *ad hoc* corrected-effec-

TABLE III. Values of the atomic-electron screening factors $\sigma^{HFS}(E_+)/\sigma^c(E_+)$ and σ^{HFS}/σ^c for $Z = 92$, $k = 3.0$ and 10.00 ($m_e c^2$). Symbols HFS and c refer to the Kohn–Sham and the point-Coulomb potentials, respectively.

	$\sigma^{HFS}(E_+)/\sigma^c(E_+)$	
y	$k = 3.00$	$k = 10.00$
0.1	4.14	1.04
0.3	1.22	1.002
0.5	1.07	1.00
0.7	1.02	1.00
0.9	0.992	0.993
σ^{HFS}/σ^c	1.05	1.003

TABLE IV. Total pair-production cross sections σ for the Kohn–Sham (HFS) potential obtained with the atomic-electron screening factor, such as shown in Fig. 5, the screened results of EST and CNST, and the point-Coulomb results of Øverbø.

	σ^{HFS} (b/atom)					
$k(m_ec^2)$	$Z=13$	$Z=29$	$Z=53$	$Z=68$	$Z=82$	$Z=92$
2.10	2.84×10^{-5}	1.94×10^{-4}	6.25×10^{-4}	8.78×10^{-4}	1.01×10^{-3}	1.03×10^{-3}
2.15	8.43×10^{-5}	5.83×10^{-4}	2.26×10^{-3}	3.50×10^{-3}	4.50×10^{-3}	5.53×10^{-3}
2.20	1.80×10^{-4}	1.21×10^{-3}	5.17×10^{-3}	8.84×10^{-3}	1.26×10^{-2}	1.51×10^{-2}
2.25	3.23×10^{-4}	2.12×10^{-3}	9.63×10^{-3}	1.75×10^{-2}	2.61×10^{-2}	3.23×10^{-2}
2.30	5.17×10^{-4}	3.31×10^{-3}	1.54×10^{-2}	2.91×10^{-2}	4.49×10^{-2}	5.70×10^{-2}
2.35	7.66×10^{-4}	4.78×10^{-3}	2.25×10^{-2}	4.35×10^{-2}	6.93×10^{-2}	8.89×10^{-2}
2.40	1.07×10^{-3}	6.53×10^{-3}	3.09×10^{-2}	6.05×10^{-2}	9.79×10^{-2}	1.29×10^{-1}
2.45	1.43×10^{-3}	8.60×10^{-3}	4.03×10^{-2}	7.96×10^{-2}	1.31×10^{-1}	1.76×10^{-1}
2.50	1.85×10^{-3}	1.09×10^{-2}	5.07×10^{-2}	1.01×10^{-1}	1.68×10^{-1}	2.28×10^{-1}
2.60	2.85×10^{-3}	1.65×10^{-2}	7.51×10^{-2}	1.49×10^{-1}	2.52×10^{-1}	3.51×10^{-1}
2.70	4.06×10^{-3}	2.31×10^{-2}	1.04×10^{-1}	2.06×10^{-1}	3.50×10^{-1}	4.93×10^{-1}
2.80	5.46×10^{-3}	3.07×10^{-2}	1.36×10^{-1}	2.69×10^{-1}	4.59×10^{-1}	6.44×10^{-1}
2.90	7.06×10^{-3}	3.93×10^{-2}	1.71×10^{-1}	3.38×10^{-1}	5.75×10^{-1}	8.04×10^{-1}
3.00	8.81×10^{-3}	4.86×10^{-2}	2.08×10^{-1}	4.09×10^{-1}	6.96×10^{-1}	9.68×10^{-1}
3.25	1.38×10^{-2}	7.49×10^{-2}	3.10×10^{-1}	6.01×10^{-1}	1.01	1.39
3.50	1.96×10^{-2}	1.05×10^{-1}	4.23×10^{-1}	8.07×10^{-1}	1.34	1.83
3.75	2.58×10^{-2}	1.37×10^{-1}	5.41×10^{-1}	1.02	1.66	2.26
4.00	3.25×10^{-2}	1.71×10^{-1}	6.64×10^{-1}	1.23	1.99	2.70
4.25	3.93×10^{-2}	2.06×10^{-1}	7.85×10^{-1}	1.44	2.30	3.10
4.50	4.64×10^{-2}	2.42×10^{-1}	9.10×10^{-1}	1.65	2.61	3.49
4.75	5.36×10^{-2}	2.78×10^{-1}	1.03	1.85	2.90	3.86
5.00	6.07×10^{-2}	3.14×10^{-1}	1.15	2.05	3.20	4.21
5.50	...	3.86×10^{-1}	1.40	2.44	3.76	4.88
6.00	...	4.57×10^{-1}	1.63	2.82	4.28	5.51
6.50	...	5.26×10^{-1}	1.86	3.17	4.78	6.11
7.00	...	5.93×10^{-1}	2.07	3.52	5.24	6.69
7.50	...	6.58×10^{-1}	2.28	3.85	5.71	7.21
8.00	...	7.20×10^{-1}	2.49	4.16	6.13	7.72
8.50	...	...	...	4.45	6.53	8.22
9.00	...	...	...	4.75	6.92	8.67
9.50	...	...	...	5.04	7.30	9.11
10.00	...	...	...	5.30	7.68	9.57

tive-normalization screening theory (CNST), which reproduced numerical results. The agreement for the total cross section is also very good, as shown in Table II. For higher-photon-energy regions the computer time needed to do exact calculations is large, and we give only some sample results. For $Z=79$, $k=2.615$ MeV ($\cong 5.117 m_ec^2$), with the energy-shift screening theory we obtained the pair-production cross sections $\sigma(E_+)=193$ and 197 $\mu b/m_ec^2$ for the HFS potential, with

$$y\equiv(E_+-1)/(k-2)=0.7 \text{ and } 0.5,$$

respectively, while the exact calculated results are 192.2 and 195.6 $\mu b/m_ec^2$, respectively. As we can see, the agreement is good.

With this energy-shift screening theory we can easily convert all the point-Coulomb pair-production results of ØMO and Øverbø[3] for incident photon energies in the range $3.0m_ec^2-10.0m_ec^2$. Sample results for $\sigma(E_+)$ are given in Figs. 2–4. Using these results and the results we obtained previously, we present in Fig. 5 the ratio σ^{HFS}/σ^c, i.e., the atomic-electron screening effect on the pair-production total cross sections. From Fig. 5 we see that the screening effect is not important for photon energies $k>3m_ec^2$ if one is interested only in pair-production total cross sections. However, if one is interested in the pair-production energy distributions $\sigma(E_+)$, the screening effect is still important in this energy region, particularly when the electron takes more of the energy, as shown in Table III for $Z=92$ and $k=3.0$ and $10.0\ m_ec^2$. We can see from Figs. 1–4 that at low energies screening increases cross sections in most parts of the energy spectrum, but with increasing energies an increasing section of the spectrum (where the positron takes more of the energy) is decreased by screening. In the total cross section, owing to cancellation between these two sections of the spectrum, there is a large energy region for which screening is not important. Using the ratio σ^{HFS}/σ^c, the results of EST and CNST,[6] and the results of ØMO and Øverbø,[3] we present a tabulation, Table IV, of the pair-

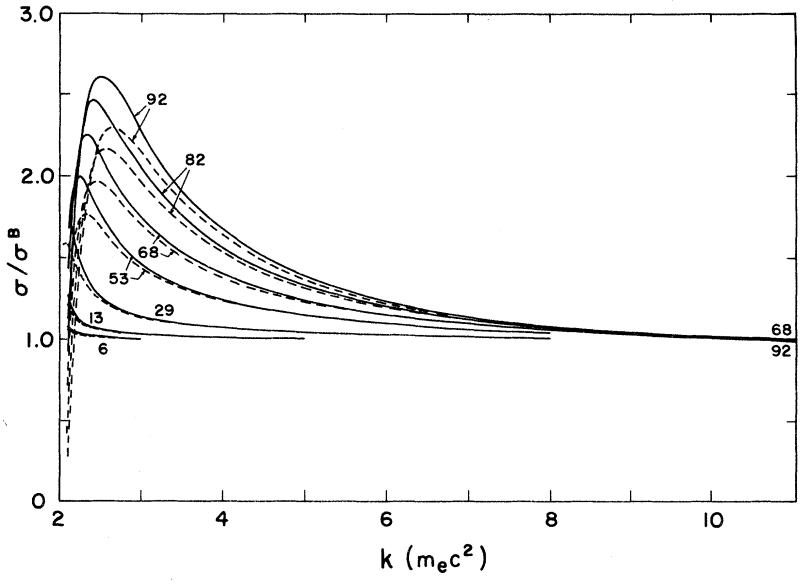

FIG. 6. Values of the ratios σ^{HFS}/σ^{B} (solid line) and σ^{c}/σ_{B} (broken line). The numbers attached to the curves give the atomic number of the target element.

production total cross section for photon energies 1.07–5.11 MeV and target elements of $Z = 13$, 29, 53, 68, 82, and 92. We then show the ratio σ^{HFS}/σ_{B} to Born approximation[2] in Fig. 6. This ratio σ^{HFS}/σ_{B} gives a combined effect of the higher Born-approximation corrections (Coulomb effects) and the atomic-electron screening effects. For comparison, we have also shown the ratio σ^{c}/σ_{B} in Fig. 6. Note that for high energies this ratio drops below one, as discussed by Bethe and Maximon.[1] We see that σ^{HFS}/σ_{B} is primarily a Coulomb effect for high photon energies, $k > 3m_{e}c^{2}$. For low photon energies, $k < 3m_{e}c^{2}$, the screening effects play an important role. σ_{HFS}/σ_{B} drops more slowly than σ_{c}/σ_{B} as the photon energy decreases because the atomic electrons decrease the Coulomb repulsion of the positrons.

Experimental studies of atomic-pair-production cross sections have been summarized by Motz, Olsen, and Koch,[9] and by Øverbø.[3] Only total cross-section data is available for the energies considered here. Two classes of experiments may be distinguished: total attenuation experiments and "direct" experiments. In total attenuation experiments one uses a narrowly collimated radiation source, allows the transmission of radiation through a thin-target slab, and uses a narrowly collimated detector to gather the transmitted radiation. From the total attenuation cross section one obtains the total pair-production cross section by subtracting the cross sections for competing attenuation mechanisms, such as scattering and photoeffect. This method thus depends on the knowledge of cross sections for other pro-

TABLE V. Comparisons between theory and the experimental data of Henry and Kennett (HK) for lead ($Z = 82$) from photon energy $k = 1.778$–5.542 MeV. Symbols HFS and expt refer to the Kohn–Sham potential and the experimental results, respectively.

k (MeV)	ØMO (semiempirical) $b^2 = 16.7$	$b^2 = 16.8$	σ^{c}	σ^{HFS} (b/atom)	σ^{expt} (HK)	$\sigma^{expt}/\sigma^{HFS}$
1.778			1.29	1.32	0.9 ± 0.3	0.68 ± 0.23
1.888			1.56	1.59	1.4 ± 0.3	0.88 ± 0.19
2.225			2.41	2.43	2.2 ± 0.3	0.91 ± 0.12
2.519			3.10	3.12	2.6 ± 0.3	0.83 ± 0.10
2.754			3.62	3.64	3.1 ± 0.3	0.85 ± 0.08
3.098			4.32	4.34	4.0 ± 0.2	0.92 ± 0.05
3.530	4.92	4.95	5.15	5.16	4.7 ± 0.2	0.91 ± 0.04
3.675	5.15	5.18	5.41	5.43	5.1 ± 0.2	0.94 ± 0.04
3.982	5.64	5.67	5.95	5.96	5.5 ± 0.2	0.92 ± 0.03
4.508	6.44	6.46	6.76	6.77	6.4 ± 0.2	0.95 ± 0.03
4.945	7.06	7.09	7.42	7.44	6.9 ± 0.2	0.93 ± 0.03
5.278	7.52	7.54	7.91	7.93	7.5 ± 0.2	0.95 ± 0.03
5.542	7.87	7.89	8.32	8.34	8.0 ± 0.2	0.96 ± 0.02

TABLE VI. Comparisons between theory and experiments for the total pair-production cross sections σ.

k (MeV)	Z	Photon source	σ^c	σ^{HFS} (mb/atom)	σ^{expt}	Ref.	$\sigma^{expt}/\sigma^{HFS}$
1.0770	53	Rb^{86}	0.543	0.800	1.1 ± 0.4	a	1.38 ± 0.50
1.099 27	53	Fe^{59}	1.82	2.32	2.2 ± 0.3	a	0.95 ± 0.13
1.115 45	53	Zn^{65}	3.36	4.00	3.8 ± 0.4	a	0.95 ± 0.10
	82		6.04	9.43	13.4 ± 1.0	b	1.42 ± 0.11
1.173 23	6	Co^{60}	0.0994	0.100	0.116 ± 0.005	c	1.16 ± 0.05
	53		13.4	14.9	13.6 ± 0.5	c	0.91 ± 0.03
	53		13.4	14.9	10.6 ± 1.9	a	0.71 ± 0.13
1.291 58	53	Fe^{59}	55.2	57.2	44.2 ± 6.2	a	0.77 ± 0.11
1.332 51	6	Co^{60}	0.602	0.602	0.603 ± 0.018	c	1.00 ± 0.03
	53		75.2	77.4	68.1 ± 1.7	c	0.88 ± 0.02
	53		75.2	77.4	60.4 ± 7.0	a	0.78 ± 0.09
1.368 55	53	Na^{24}	95.3	97.4	86.4 ± 15	a	0.89 ± 0.15
2.614 66	13	Th C''	64.1	64.1	59.0 ± 10.0	d	0.92 ± 0.16
2.754 10	53	Na^{24}	1340	1350	1394 ± 190	a	1.03 ± 0.14
	82		3620	3640	3430 ± 700	b	0.94 ± 0.19
	82		3620	3640	2380 ± 620	e	0.65 ± 0.17
	82		3620	3640	3180 ± 120	f	0.87 ± 0.03

[a] J. Huck, Ref. 12.
[b] S. Standil and V. Shkolnik, Ref. 11.
[c] H. I. West, Jr., Ref. 12.
[d] F. Titus and A. J. Levy, Ref. 13.
[e] S. Standil and R. D. Moore, Ref. 11.
[f] P. Schmid and P. Huber, Ref. 11.

cesses and is most satisfactory when pair production dominates the total attenuation cross section, namely, for high photon energies. Many experimental studies of this type have been made. In the photon-energy range below 5 MeV results have been reported by Davisson and Evans, by Colgate, by Rosenblum, Schrader, and Warner, by Barlett and Donahue, by Barkan, and by Henry and Kennett (HK).[10] Comparisons between our predictions and the experimental data of HK for $Z = 82$ are given in Table V. Note that atomic-electron screening effects are unimportant for this data. In Table V we also show the results of the semiempirical formula of Øverbø, Mork, and Olsen[3] with $b^2 = 16.7$ and 16.8, namely,

$$\sigma = \sigma_B - 4.02 + (b^2/k)\ln(k - 0.75)\ \text{b/atom},$$

for lead. The difference between the results with $b^2 = 16.7$ and 16.8 is very small. There is about a 5% difference between the results of this semiempirical formula and the point-Coulomb results.

Some direct experiments have used two scintillation counters to detect annihilation events following pair production, as reported by Hahn, Baldinger, and Huber, by Dayton, by Schmid and Huber, by Staub and Winkler, by Standil and Moore, by Standil and Shkolnik, and by Rao *et al.*[11] The disadvantage of this method is that, when using a radiation source emitting γ rays of more than one energy above the threshold, the equipment accepts all pair-production events without discriminating photon energies. A modification of the method, using a three-crystal scintillation pair spectrometer to obtain relative pair-production cross sections, has been used by Griffiths and Warren, by West, by Singh, Dosso, and Griffiths, by Huck, and by Yamazaki and Hollan-

TABLE VII. Comparisons between theory and experiments for the value of σ/σ_B.

k (MeV)	Z	Photon source	σ^c/σ_B	σ^{HFS}/σ_B	σ^{expt}/σ_B	Ref.	$\sigma^{expt}/\sigma^{HFS}$
1.332 51	13	Co^{60}	1.05	1.05	1.03 ± 0.03	a	0.98 ± 0.03
	29		1.21	1.22	1.14 ± 0.04	a	0.93 ± 0.03
	82		2.18	2.33	2.04 ± 0.06	a	0.88 ± 0.03
	82		2.18	2.33	2.08 ± 0.22	b	0.89 ± 0.09
2.614 66	13	Th C''	1.008	1.008	1.006 ± 0.002	a	0.998 ± 0.002
	29		1.05	1.05	1.03 ± 0.02	a	0.98 ± 0.02
	82		1.31	1.32	1.23 ± 0.03	a	0.93 ± 0.02
	82		1.31	1.32	1.33 ± 0.03	b	1.01 ± 0.02

[a] I. E. Dayton, Ref. 11.
[b] B. Hahn, E. Baldinger, and P. Huber, Ref. 11.

TABLE VIII. Comparisons between theory and experiments for the relative total pair-production cross sections $\sigma(k_1)/\sigma(k_2)$, where k_1 and k_2 are photon energies. Symbols HFS, Coul., and Bonn refer to the Kohn–Sham potential, the point-Coulomb potential, and the Bonn approximation, respectively.

		$\frac{\sigma(1.17323)}{\sigma(1.11545)}$ $Z=53$	$\frac{\sigma(1.33251)}{\sigma(1.17323)}$ $Z=6$	$Z=53$	$\frac{\sigma(2.61466)}{\sigma(1.33251)}$ $Z=53$	$\frac{\sigma(2.75410)}{\sigma(1.36855)}$ $Z=53$
Expt.	a	4.22 ± 0.32	...	5.10 ± 0.38	16.8 ± 1.3	...
	b	...	5.20 ± 0.17	5.00 ± 0.15	...	15.0 ± 0.8
	c	...	...	5.2 ± 1.5	...	14.5 ± 2.5
Theory	Coul.	3.70	6.13	6.13	22.8	19.8
	d	3.99	6.06	5.61	16.1	14.1
	HFS	3.73	6.02	5.19	15.6	13.9

[a]P. P. Singh, H. W. Dosso, and G. M. Griffiths, Ref. 12.

[b]H. I. West, Jr. Ref. 12.

[c]G. M. Griffiths and J. B. Warren, Ref. 12.

der.[12] Another approach used by Titus and Levy[13] is to measure the pair-production cross section in terms of the differential Compton-scattering cross section at the same photon energy. Comparisons between the results of theory and these experiments are given in Tables VI–VIII. In the lower-energy data screening effects are becoming important even for total cross sections. Note that the point-Coulomb results presented in Tables VI–VIII are different from those given by Øverbø,[3] especially for very low photon energies. For example, for $Z=53$ with photon source Rb^{86} our $\sigma^c = 0.543$ mb, but the result of Øverbø is 0.662 mb. This is because Øverbø did not use the more precise photon energies now available, i.e., k should be 1.0770 MeV instead of 1.080 MeV. The photon energies in Tables VI–VIII are obtained from the recent compilation of Martin and Blichert-Toft.[14]

*Work supported in part by the National Science Foundation under Grant No. GP-32798.

[1]H. A. Bethe and L. C. Maximon, Phys. Rev. 93, 768 (1954); H. Olsen, L. C. Maximon, and H. Wergeland, *ibid.* 106, 27 (1957); H. Olsen and L. C. Maximon, *ibid.* 114, 887 (1957); A. Sørenssen, Nuovo Cimento 38, 745 (1965); 41, 543 (1966).

[2]H. A. Bethe and W. Heitler, Proc. Roy. Soc. (London) A146, 83 (1934); F. Sauter, Ann. Physik 20, 404 (1934); G. Racah, Nuovo Cimento 11, 461 (1934); 11, 467 (1934).

[3]I. Øverbø, K. J. Mork, and H. A. Olsen, Phys. Rev. 175, 1978 (1968); I. Øverbø, Arkiv for Det Fysiske Seminar:Trondheim, No. 9 (1970).

[4]H. A. Bethe, Proc. Cambridge Phil. Soc. 30, 524 (1934); Ann. Physik 5, 385 (1930).

[5]W. Heitler, *The Quantum Theory of Radiation*, 3rd ed. (Oxford U. P., London, 1954), p. 249.

[6]H. K. Tseng and R. H. Pratt, Phys. Rev. A 4, 1835 (1971). We follow the same notations we used in this paper. We used the unrationalized units, i.e., $\hbar = m_e = c = 1$, throughout unless specified.

[7]R. H. Pratt and H. K. Tseng, Phys. Rev. A 5, 1063 (1972).

[8]W. Kohn and L. S. Sham, Phys. Rev. 140, A1133 (1965); D. A. Liberman, D. T. Cromer, and J. T. Waber, Computer Phys. Commun. 2, 107 (1971). We wish to thank Dr. Liberman for kindly sending us the relativistic–self-consistent–field computer code for calculating the potentials.

[9]J. W. Motz, H. A. Olsen, and H. W. Koch, Rev. Mod. Phys. 41, 581 (1969).

[10]C. M. Davisson and R. D. Evans, Phys. Rev. 81, 404 (1951); S. A. Colgate, *ibid.* 87, 592 (1952); E. S. Rosenblum, E. F. Schrader, and R. M. Warner, Jr., *ibid.* 88, 612 (1952); R. H. Barlett and D. J. Donahue, *ibid.* 137, A523 (1965); S. M. Barkan, Phys. Rev. A 1, 1022 (1970); L. C. Henry and T. J. Kennett, Can. J. Phys. 49, 1167 (1971).

[11]B. Hahn, E. Baldinger, and P. Huber, Helv. Phys. Acta 25, 505 (1952); I. E. Dayton, Phys. Rev. 89, 544 (1953); P. Schmid and P. Huber, Helv. Phys. Acta 27, 152 (1954); 28, 389 (1955); H. Staub and H. Winkler, *ibid.* 27, 223 (1954); S. Standil and R. D. Moore, Can. J. Phys. 34, 1126 (1956); S. Standil and V. Shkolnik, *ibid.* 36, 1154 (1958); J. R. Rao, V. Lakshminarayana, and S. Jnanananda, Proc. Roy. Soc. (London) 81, 949 (1963); Indian J. Pure Appl. Phys. 1, 199 (1963).

[12]G. M. Griffiths and J. B. Warren, Proc. Phys. Soc. (London) A65, 1050 (1952); H. I. West, Jr., Phys. Rev. 101, 915 (1956); P. P. Singh, H. W. Dosso, and G. M. Griffiths, Can. J. Phys. 37, 1055 (1959); J. Huck, Phys. Radium 25, 1029 (1964); T. Yamazaki and J. M. Hollander, Phys. Rev. 140, B630 (1965).

[13]F. Titus and A. J. Levy, Nucl. Phys. 80, 588 (1966).

[14]M. J. Martin and P. H. Blichert-Toft, Nucl. Data Tables A8, 1 (1970).